

Excited State Proton Transfer in Guanine in the Gas Phase and in Water Solution: A Theoretical Study

M. K. Shukla and Jerzy Leszczynski*

Computational Centre for Molecular Structure and Interactions, Department of Chemistry, Jackson State University, Jackson, Mississippi 39217

Received: May 5, 2005; In Final Form: July 7, 2005

Theoretical investigations were performed to study the phenomena of ground and electronic excited state proton transfer in the isolated and monohydrated forms of guanine. Ground and transition state geometries were optimized at both the B3LYP/6-311++G(d,p) and HF/6-311G(d,p) levels. The geometries of tautomers including those of transition states corresponding to the proton transfer from the keto to the enol form of guanine were also optimized in the lowest singlet $\pi\pi^*$ excited state using the configuration interaction singles (CIS) method and the 6-311G(d,p) basis set. The time-dependent density function theory method augmented with the B3LYP functional (TD-B3LYP) and the 6-311++G(d,p) basis set was used to compute vertical transition energies using the B3LYP/6-311++G(d,p) geometries. The TD-B3LYP/6-311++G(d,p) calculations were also performed using the CIS/6-311G(d,p) geometries to predict the adiabatic transition energies of different tautomers and the excited state proton transfer barrier heights of guanine tautomerization. The effect of the bulk aqueous environment was considered using the polarizable continuum model (PCM). The harmonic vibrational frequency calculations were performed to ascertain the nature of potential energy surfaces. The excited state geometries including that of transition states were found to be largely nonplanar. The nonplanar fragment was mostly localized in the six-membered ring. Geometries of the hydrated transition states in the ground and lowest singlet $\pi\pi^*$ excited states were found to be zwitterionic in which the water molecule is in the form of hydronium cation (H_3O^+) and guanine is in the anionic form, except for the N9H form in the excited state where water molecule is in the hydroxyl anionic form (OH^-) and the guanine is in the cationic form. It was found that proton transfer is characterized by a high barrier height both in the gas phase and in the bulk water solution. The explicit inclusion of a water molecule in the proton transfer reaction path reduces the barrier height drastically. The excited state barrier height was generally found to be increased as compared to that in the ground state. On the basis of the current theoretical calculation it appears that the singlet electronic excitation of guanine may not facilitate the excited state proton transfer corresponding to the tautomerization of the keto to the enol form.

1. Introduction

Guanine is one of the most important building blocks of nucleic acid in living systems. It has the maximum number of minor tautomers in different environments and is the most reactive site for oxidative damages. Therefore, it is not surprising that guanine has been the subject of numerous experimental¹ and theoretical² investigations. Both experimental and theoretical methods have predicted the existence of several tautomers in the gas phase and in aqueous media.^{1,2} There is some contradiction in the relative stability of guanine tautomers in the ground state. It has been shown that the basis set has an appreciable effect on the relative stability of the different tautomers of guanine.^{2h} Thus, at the MP2/6-31G(d,p) level the keto-N7H form of guanine is predicted to be the most stable in the gas phase, but at the MP2/6-311G(d,p)/MP2/6-31G(d,p) level the keto-N9H form is revealed to be the most stable tautomer.^{2h} However, at the MP2/6-311++G(df,pd)/MP2/6-31G(d,p) level, the enol-N9H form of guanine is found to be the most stable tautomer in the gas phase.^{2h}

Recently, several high levels of spectroscopic investigations were performed on guanine and its derivatives in the supersonic

jet expansion to unravel the structural and dynamical properties of the molecule.³ Although the guanine absorbs the UV-radiation efficiently, the quantum efficiency of emission is very poor.^{1d} The most parts of the absorbed radiation are released in the form of nonradiative processes, which are generally believed to be internal conversion in the subpicosecond time scale.^{1a,4} The existence of up to four tautomers of guanine has been detected in the supersonic beam experiments.⁵ Recently appearing results from two groups are worth mentioning in this context. Nir et al.^{5a} have performed a jet-cooled spectroscopic study on guanine and suggested the existence of three tautomers, namely, enol-N9H (32870), keto-N7H (33274), and keto-N9H (33914) of the molecule. Mons et al.^{5b} have performed a similar study on guanine and have shown the existence of four tautomers, namely, enol-N7H (32864), keto-N7H (33269), keto-N9H (33910), and enol-N9H (34755). The numbers in parentheses for both of the above-mentioned studies are the spectral origin (0–0 transition) for the lowest singlet $\pi\pi^*$ excited state. Therefore, these results are not consistent with respect to the spectral origin of enol tautomers. To resolve this ambiguity, one has to optimize the ground and lowest singlet $\pi\pi^*$ excited state geometries of all four tautomers of guanine. Further, the excited state geometries of complex molecule like guanine

* Corresponding author. E-mail: jerzy@ccmsi.us.

cannot be determined experimentally. Only a few theoretical calculations based on single reference methods are available.⁶ These investigations have suggested the nonplanar excited state geometries of guanine tautomers.

Theoretically, the ground state barrier height corresponding to the keto–enol tautomerization of the guanine is predicted to be very high.^{2b,7} The presence of a water molecule in the proton-transfer reaction path is found to reduce the barrier height of proton transfer very significantly.^{2b,7} The barrier height of the proton transfer in the excited state of guanine has not yet been investigated. This type of study is very significant, because in some model systems the proton transfer in the excited state is predicted to proceed through a significantly low barrier or to be even barrierless.⁸ In this paper, we have used the TD-DFT method⁹ using the B3LYP functional in combination with the CIS method¹⁰ to resolve the ambiguity of the spectral origin of guanine tautomers. Further, excited state proton transfer and the effect of hydration on the proton-transfer barrier height in the gas phase and in the bulk water solution are also investigated.

2. Computational Details

The ground state geometry of four tautomers of guanine (keto-N9H, keto-N7H, enol-N9H, and enol-N7H), their monohydrated forms, and the transition states corresponding to the proton transfer from the keto to the enol form were optimized at the B3LYP level using the 6-311++G(d,p) basis set. The geometries in the lowest singlet $\pi\pi^*$ electronic excited states were optimized at the CIS level using the 6-311G(d,p) basis set. To compare with the excited state geometrical parameters, the ground state geometries were also optimized at the HF/6-311G(d,p) level. The nature of potential energy surface was ascertained using the harmonic vibrational frequency analysis. The vertical singlet electronic transition energies of different tautomers were computed using the TD-DFT method employing the B3LYP functional and the 6-311++G(d,p) basis set using the DFT optimized ground state geometries. To compute adiabatic transition energies, the vertical transition energy calculation were also performed at the TD-B3LYP/6-311++G(d,p) level using the excited state optimized geometries. The effect of aqueous solution on the ground and excited state energies were considered using the polarizable continuum (PCM) model.^{6c,11} All calculations were performed using the Gaussian 03 suite of programs.¹² The molecular orbitals were visualized using the Molekel program.¹³

3. Results and Discussion

The ground state geometries of guanine tautomers namely keto-N9H, keto-N7H, enol-N9H, and enol-N7H are revealed to be planar, except for the amino group, which is pyramidal.² The atomic numbering scheme of guanine is presented in the Figure 1. Guanine has been subject of several experimental and theoretical investigations in the ground state.^{16,2} Therefore, we will discuss here mainly excited state properties such as electronic transitions, the transition state in the excited state, and geometries.

3.1. Relative Stability and Electronic Transitions. The ground state geometries of the four tautomers of guanine namely keto-N9H, keto-N7H, enol-N9H, and enol-N7H (see Figure 1 for the atomic numbering schemes) were optimized at the HF/6-311G(d,p) and B3LYP/6-311++G(d,p) levels. The relative total energy of tautomers in the gas phase and in water solution at the B3LYP/6-311++G(d,p) level is presented in the Table 1. It is evident from Table 1 that the keto-N7H tautomer is the most stable in the gas phase and the keto-N9H tautomer is the

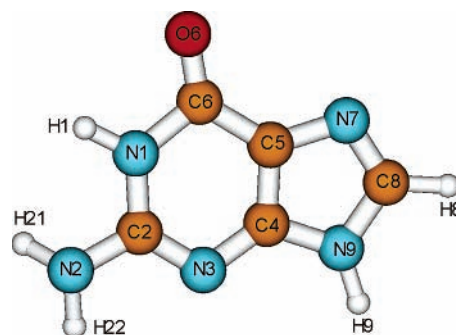


Figure 1. Atomic numbering schemes in guanine (keto-N9H). The keto-N7H, enol-N9H, and enol-N7H tautomers of guanine can be obtained by moving H9 hydrogen to N7 site, H1 hydrogen to the O6 site, and H1 hydrogen to the O6 site of the keto-N7H tautomer, respectively.

TABLE 1: Relative Energy (ΔE , kcal/mol) and Adiabatic Transition Energy (0–0 Transition, cm^{-1}) for the Lowest Singlet $\pi\pi^*$ Excited State of Guanine Tautomers in the Gas Phase and in Aqueous Solution^a

tautomer	ΔE		adiabatic transition energy		
	gas	water	gas	water	experimental
K–N9H	0.0	0.0	34866	36746	33910
K–N7H	–0.44	0.53	35820	36555	33269
E–N9H	1.27	7.00	36509	36000	34755
E–N7H	4.21	8.44	34177	34550	32864

^a Ground state energies are at the B3LYP/6-311++G(d,p) level, adiabatic transition energies are at the TD-B3LYP/6-311++G(d,p)//CIS/6-311G(d,p) level (for detailed explanation see text), effect of water solution was modeled using PCM model, and for the experimental adiabatic transition energies, see ref 5b.

TABLE 2: Computed and Observed Transition Energies (ΔE) and Oscillator Strengths (f) of the keto-N9H and keto-N7H Tautomers of Guanine in the Gas Phase and in Water Solution at the TD-B3LYP/6-311++G(d,p)//B3LYP/6-311++G(d,p) Level

gas phase		water solution		CASPT2/CASSCF ^a $\Delta E^1/\Delta E^2/f$	observed ^b ΔE
ΔE	f	ΔE	f		
keto-N9H					
$\pi\pi^*$ transitions					
4.88	0.1219	4.82	0.1441	4.76/6.08/0.113	4.4–4.6
5.18	0.2241	5.18	0.3626	5.09/6.99/0.231	4.8–5.1
$n\pi^*$ transitions					
5.30	0.0017	5.64	0.0001	5.79/6.22	5.21
keto-N7H					
$\pi\pi^*$ transitions					
4.62	0.1121	4.54	0.1481		
5.37	0.0972	5.39	0.1828		
$n\pi^*$ transitions					
5.06	0.0004	5.35	0.0009		

^a ΔE^1 is the CASPT2 and ΔE^2 is the CASSCF energy.¹⁵ ^b Observed experimental range of transition energies.^{1d,2a,i,14}

most stable in the water solution. A large destabilization of the stability of the enol-N9H tautomer was revealed in going from the gas phase to aqueous solution. These results are in agreement with different experimental and theoretical results, suggesting the preferential stability of the keto-N7H tautomer in the gas phase and the keto-N9H tautomer in the water solution.^{1i,j,2,6c}

The computed vertical singlet transition energies corresponding to the lowest two $\pi\pi^*$ and lowest $n\pi^*$ transitions of the keto-N9H and keto-N7H tautomers of guanine obtained at the TD-B3LYP/6-311++G(d,p)//B3LYP/6-311++G(d,p) level are shown in the Table 2. The experimental transition energies^{1d,2a,i,14} and transitions computed at the CASPT2 level¹⁵ are also shown

in the same table for the comparison. In the case of the keto-N9H tautomer, the TD-B3LYP method predicts first singlet $\pi\pi^*$ transition near 4.8 eV and second transition near 5.2 eV in the water solution (Table 2). The intensity of the second transition is larger than that of the first transition. Different experimental investigations suggest that the first transition of guanine is in the range 4.4–4.6 eV, with the second transition observed in the range 4.8–5.1 eV. The intensity of the first transition is weaker than the intensity of the second transition. The CASPT2 computed transition energies are predicted near 4.8 and 5.1 eV.¹⁵ Therefore, our computed transition energies are in good agreement with the experimental data and the CASPT2 results. Our calculation has suggested the existence of the lowest singlet $n\pi^*$ transition near 5.3 eV in the gas phase and near 5.6 eV in the water solution of guanine. Experimentally, Clark has tentatively suggested the existence of the first $n\pi^*$ transition near 5.2 eV in guanine.^{14c} With regard to the keto-N7H tautomer, the first two singlet vertical $\pi\pi^*$ transitions are predicted near 4.6 and 5.4 eV in the gas phase and near 4.5 and 5.4 eV in the water solution. Thus, the lowest singlet vertical $\pi\pi^*$ transition of the keto-N7H tautomer in the gas phase and in water solution is red-shifted than the corresponding transition of the keto-N9H tautomer. This prediction is in agreement with the experimental result that the first absorption band of 7-methylguanine is about 10 nm red-shifted than the corresponding absorption band of the guanosine monophosphate (GMP).¹⁶ An elaborated description of several absorption transitions of guanine can be found in our recent publication where a detailed study about vertical transitions of nucleic acid bases obtained at the TD-DFT level with different large basis sets including several sets of diffuse functions are reported.²¹

The computed adiabatic transition energies of the guanine tautomers corresponding to the lowest singlet $\pi\pi^*$ excited state in the gas phase and in water solution are also presented in the Table 1 along with the experimental data in the gas phase.^{5b} The adiabatic transition energies were obtained by taking the energy difference between the separately optimized ground and excited state geometries at the B3LYP/6-311++G(d,p) and TD-B3LYP/6-311++G(d,p)//CIS/6-311G(d,p) levels, respectively. There appears to be a qualitative agreement between the theoretical and experimental data. The theoretical prediction that the enol-N9H tautomer would have the largest and the enol-N7H tautomer would have lowest adiabatic transition energy is in agreement with the experimental data. The disagreement is revealed with respect to the keto tautomers. The experimental results suggest that the keto-N9H tautomer has a larger adiabatic transition energy than the keto-N7H tautomer; the contradictory result is revealed by the theoretical calculation in the gas phase (Table 1). It should be noted that the CIS method was used for the excited state geometry optimization and the TD-DFT method was used to compute the adiabatic transition energies utilizing the CIS optimized excited state geometries of guanine tautomers. Further, the computed accuracy of the TD-DFT method is generally in the range of 0.3–0.5 eV. Therefore, in view of the limitation of theoretical methods used in the present work, the theoretical prediction can be regarded as in good agreement with the corresponding experimental data.

3.2. Proton-Transfer Barrier Height. The computed proton-transfer barrier heights corresponding to the proton transfer from the keto to the enol tautomeric form in the gas phase and in water solution is shown in the Table 3. The proton-transfer barrier heights in the gas phase and in water solution were also computed by the inclusion of a water molecule in the proton-transfer reaction path. This table indicates that the ground state

TABLE 3: Computed Barrier Height (kcal/mol) for Guanine Corresponding to the Keto–Enol Tautomerism in the Ground and the Lowest Singlet $\pi\pi^*$ Excited State Obtained at the B3LYP/6-311++G(d,p) and TD-B3LYP/6-311++G(d,p)//CIS/6-311G(d,p) Level, Respectively in the Gas Phase and in Water Solution

species	ground state		excited state	
	gas	water	gas	water
keto-N9H \rightarrow TS–N9H	37.5	45.2	42.9	45.7
enol-N9H \rightarrow TS–N9H	36.3	38.2	36.9	40.8
keto-N7H \rightarrow TS–N7H	40.6	46.5	36.8	41.4
enol-N7H \rightarrow TS–N7H	35.9	38.5	36.8	39.3
keto-N9H.H ₂ O \rightarrow TS–N9H.H ₂ O	15.9	16.7	19.8	18.3
enol-N9H.H ₂ O \rightarrow TS–N9H.H ₂ O	12.8	10.4	12.8	13.5
keto-N7H.H ₂ O \rightarrow TS–N7H.H ₂ O	17.3	17.1	13.9	13.5
enol-N7H.H ₂ O \rightarrow TS–N7H.H ₂ O	12.0	10.2	13.4	11.2

tautomerization of guanine in the gas phase is characterized by a very high energy barrier. This result is in agreement with other theoretical results.^{2b,7} The inclusion of bulk aqueous solvation using the polarizable continuum model (PCM) further increases the tautomerization barrier height in the ground state. The inclusion of a single water molecule in the proton transfer reaction significantly reduces the gas phase ground state barrier height. However, the bulk aqueous solvation of the monohydrated system does not have a significant effect on the tautomerization barrier height in the ground state. On the other hand with few exceptions, the tautomerization barrier height was revealed to be increased in the lowest singlet $\pi\pi^*$ excited state both in the gas phase and in aqueous medium. Therefore, on the basis of the current theoretical calculation it appears that the singlet electronic excitation of guanine may not facilitate the excited state proton transfer corresponding to the tautomerization of the keto to the enol form.

3.3. Ground State, Excited State, and Transition State Geometries. Some selected geometrical parameters (amino group angles and some dihedral angles) of guanine tautomers in the ground, lowest singlet $\pi\pi^*$ excited, and transition states are shown in the Table 4. Ground state geometries of guanine tautomers were revealed to be planar except for the amino group, which was found to be pyramidal. This is in agreement with numerous theoretical calculations on the guanine at different levels of theory.^{2b,g,h,7} The deviation of amino angles from the planarity ($360^\circ - \Sigma\text{HNN}$) is a measure of the pyramidalization of the amino group. At both of the B3LYP/6-311++G(d,p) and HF/6-311G(d,p) levels of the calculation, the amino group of the keto-N7H tautomer is revealed to have the highest and the enol-N9H tautomer has the lowest pyramidal character (Table 4). The ground state geometrical parameters at the HF/6-311G(d,p) and B3LYP/6-311++G(d,p) levels are generally revealed to be similar (Table 4). It should be noted that earlier investigations have suggested that the ring geometry of nucleic acid bases are flexible and the predicted values of amino group dihedral angles are basis set and method dependent.^{2b} The geometry of guanine in the lowest singlet $\pi\pi^*$ excited state is highly nonplanar and the nonplanarity is mainly localized at the C6N1C2N3 fragment of the six-membered ring.⁶ Further, in the lowest singlet $\pi\pi^*$ excited state, the keto-N9H tautomer has the largest amino group pyramidalization among all four tautomers, which is evident from the amount of deviation of amino angles from the planarity (Table 4). The geometry of tautomers in the lowest singlet $\pi\pi^*$ excited state is shown in Figures 2 and 3 along with bond length parameters in the ground and excited state. Geometry is twisted along the N1C2 bond; the N1, C2, and C6 atoms are significantly out-of-plane. Selected ring dihedral angles and amino group angles computed at the

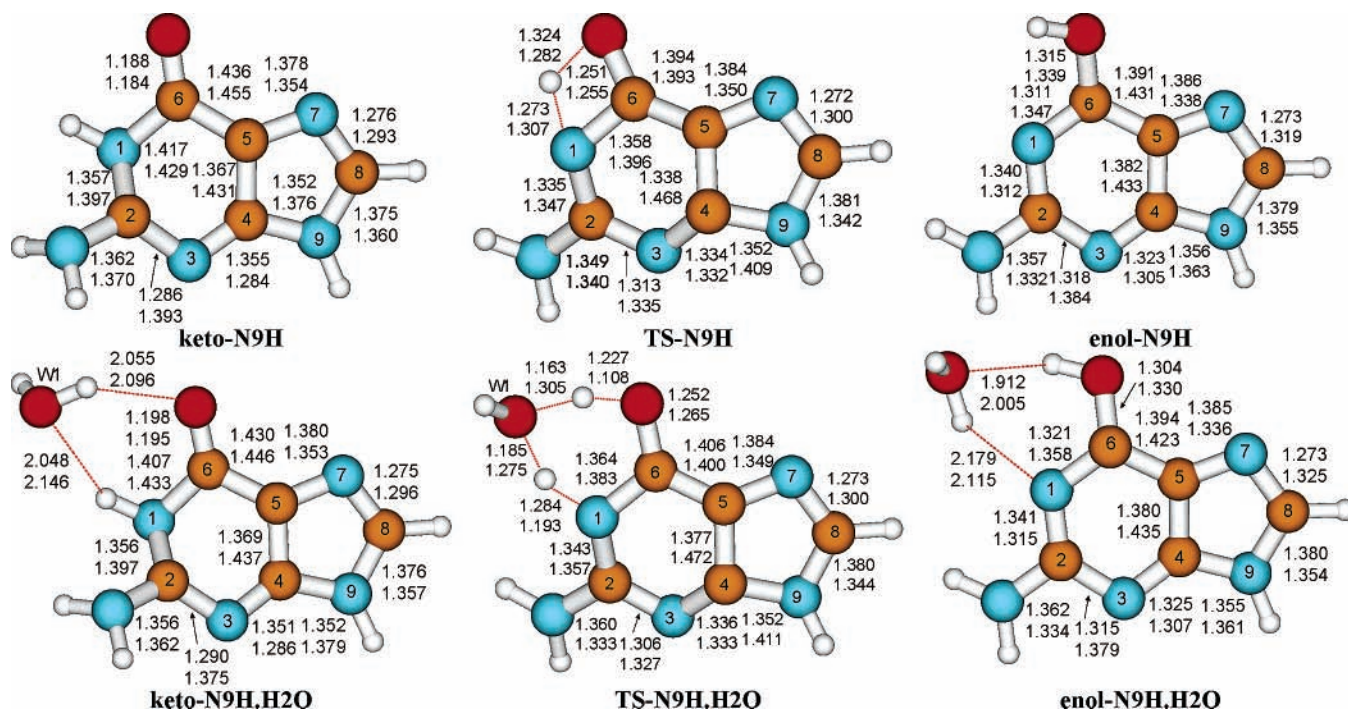


Figure 2. Lowest singlet $\pi\pi^*$ excited state geometries of the keto-N9H, enol-N9H, and transition state TS-N9H corresponding to the proton transfer from the keto to the enol tautomer in the isolated and monohydrated guanine in the gas phase. The top and bottom indices correspond to the ground and excited state obtained at the HF/6-311G(d,p) and CIS/6-311G(d,p) levels, respectively.

TABLE 4: Some Selected Geometrical Parameters of Guanine Tautomers and Transition States in the Ground and Lowest Singlet $\pi\pi^*$ Excited State at the HF/6-311G(d,p) and CIS/6-311G(d,p) Level. Parameters in Parentheses are Obtained at the B3LYP/6-31++G(d,p) Level

parameter	keto-N9H		keto-N7H		enol-N9H		enol-N7H		TS-N9H		TS-N7H	
	S0	S1	S0	S1	S0	S1	S0	S1	S0	S1	S0	S1
H21N2C2	117.9 (118.2)	115.3	116.8 (117.7)	117.3	116.9 (117.3)	119.7	116.6 (117.3)	119.6	118.5 (118.5)	118.9	118.0 (118.5)	118.9
H22N2C2	113.8 (113.8)	112.7	112.5 (112.7)	114.1	116.7 (117.1)	119.1	115.8 (116.4)	119.0	116.6 (116.4)	118.1	115.7 (115.8)	117.8
H21N2H22	115.0 (114.7)	111.4	113.8 (114.0)	114.5	118.0 (118.2)	121.2	117.3 (117.8)	121.4	118.1 (117.6)	119.2	117.5 (117.5)	119.4
360 - Σ HNH	13.3 (13.3)	20.6	16.9 (15.6)	14.1	8.4 (7.4)	0.0	10.3 (8.5)	0.0	6.8 (7.5)	3.8	8.8 (8.2)	3.9
N3C2N1C6	-0.6	-64.0	-0.5	-45.1	-0.7	1.9	-0.9	0.0	-0.6	28.8	-0.7	-21.9
C4N3C2N1	0.8	44.2	0.9	22.9	0.8	5.1	0.9	0.0	0.6	1.9	0.7	10.0
C4N3C2N2	-177.2	-161.4	-177.0	-165.3	-177.9	-175.6	-177.7	180.0	-178.1	-175.8	-177.9	-172.1
C5C4N3C2	-1.0	-2.4	-1.2	7.3	-0.3	-5.6	-0.2	0.0	-0.3	-30.8	-0.3	4.7
C6C5C4N3	0.9	-18.5	1.1	-14.4	-0.2	-0.2	-0.4	0.0	0.1	28.0	-0.1	-6.4
C5C6N1C2	0.3	36.2	0.3	32.6	0.1	-8.3	0.1	0.0	0.3	-29.9	0.3	18.5
N1C6C5C4	-0.4	-0.6	-0.6	-7.0	0.2	7.5	0.5	0.0	-0.1	3.5	0.0	-5.6
H21N2C2N1	30.4 (31.2)	42.3	36.6 (35.7)	32.3	17.2 (16.4)	-0.2	19.9 (18.3)	0.0	16.9 (18.0)	-11.1	19.9 (19.6)	13.0
H22N2C2N1	169.4 (170.2)	171.8	170.9 (171.5)	170.2	164.8 (165.8)	-178.8	164.1 (165.6)	180.0	167.4 (167.2)	-169.3	166.7 (167.4)	170.6

HF/6-311G(d,p) and CIS/6-311G(d,p) levels in the ground and excited states are shown in Table 4 for the comparison. Here it should be noted that the CIS method is the HF analogue for the excited state.¹⁰ In going from the ground state to the excited state, the dihedral angles N3C2N1C6, C4N3C2N1, C6C5C4N3, and C5C6N1C2 are changed in the range 18–65°. Similar changes were also found for the keto-N7H tautomer in the excited state. However, the amount of such change is smaller than that in the keto-N9H tautomer. The geometries of enol tautomers in the excited state were revealed to be planar. In is interesting to note that though the amino group is pyramidal in the ground state, it is also revealed to be planar in the excited state.

Selected geometrical parameters (amino angles and dihedral angles) of transition states, TS-N9H, and TS-N7H corre-

sponding to the proton transfer from the keto-N9H form to the enol-N9H form and from the keto-N7H form to the enol-N7H form, respectively, in the ground and lowest singlet $\pi\pi^*$ excited state are also shown in Table 4. The geometries of transition states in the excited state are shown in Figures 2 and 3 along with the corresponding bond distances in the ground and excited state. The structures of transition states for the hydrated tautomers, where a water molecule was placed in the proton-transfer reaction path, are also shown in the same figures. Transition state geometries in the ground state are planar except for the amino groups for both the isolated and hydrated forms, except for a hydrogen atom attached to the water molecule that is away from the molecular plane. The geometries in the lowest singlet $\pi\pi^*$ excited state were revealed to be appreciably nonplanar in the six-membered part of the ring for both the

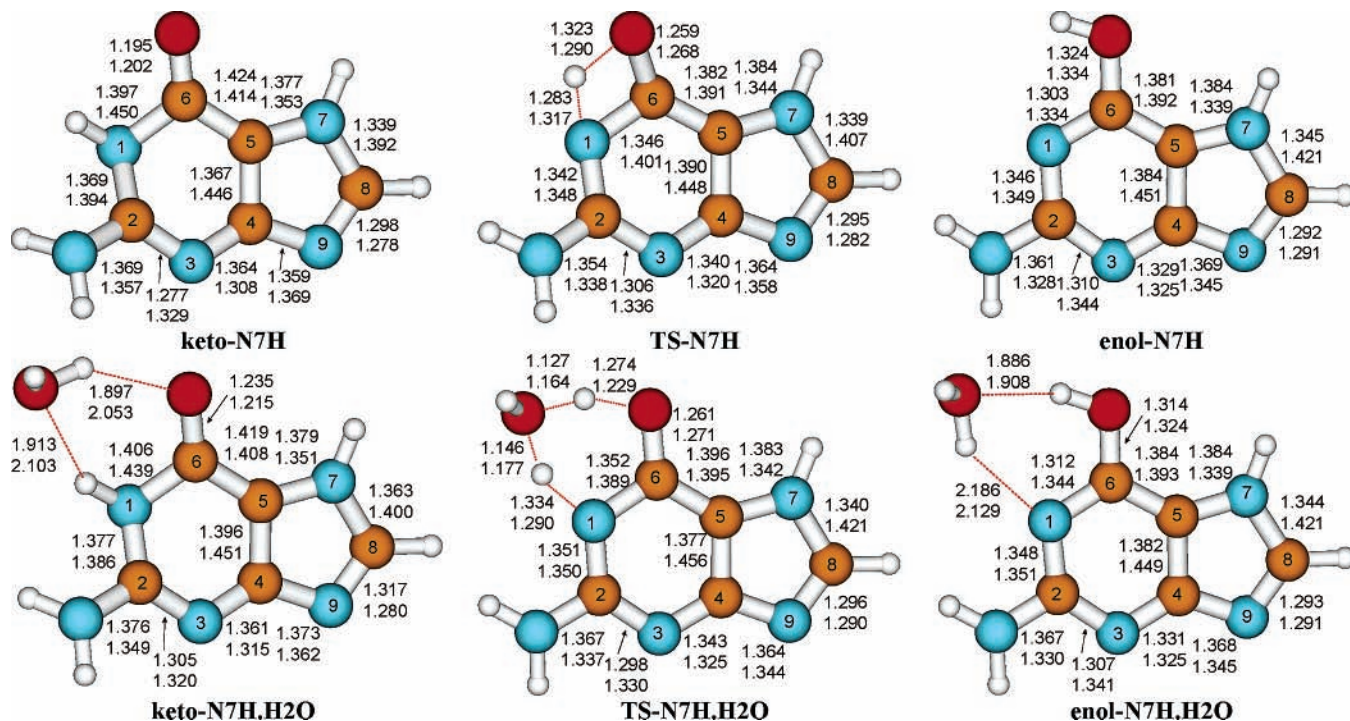


Figure 3. Lowest singlet $\pi\pi^*$ excited state geometries of the keto-N7H, enol-N7H, and transition state TS-N7H corresponding to the proton transfer from the keto to the enol tautomer in the isolated and monohydrated guanine in the gas phase. The top and bottom indices correspond to the ground and excited state obtained at the HF/6-311G(d,p) and CIS/6-311G(d,p) levels, respectively.

isolated and hydrated forms. The structural nonplanarity of the TS-N9H was revealed to be different from the keto-N9H tautomer in the lowest singlet $\pi\pi^*$ excited state (Table 4, Figure 2). For example, the N3C2N1C6 and C4N3C2N1 dihedral angles are changed from -64.0 and 44.2° to 28.8 and 1.9° , respectively, in comparing the excited state of the keto-N9H tautomer to the excited state of the TS-N9H form (Table 4). Further, the C5C4N3C2 dihedral angle is increased from 2.4 to 30.8° . The geometry of the TS-N9H tautomer in the excited state can be approximately described as the N1C2N3C4 part of the ring is folded along the N1C4 direction. Further, in going from the ground state to the excited state of the TS-N9H structure, the O6 \cdots H1 bond distance is decreased from 1.324 to 1.282 Å and the N1 \cdots H1 bond distance is increased from 1.273 to 1.307 Å (Figure 2). On the other hand, structural deformation of the TS-N7H transition state in the excited state is generally similar to the geometry of keto-N7H tautomer in the excited state, but the amount of deformation is comparatively smaller. Also, in the TS-N7H transition state, the O6 \cdots H1 bond distance is decreased by 0.033 Å and the N1 \cdots H1 bond distance is increased by about the same amount in going from the ground state to the lowest singlet $\pi\pi^*$ excited state (Figure 3).

The structural deformations of the hydrated transition state structures are generally similar to the corresponding unhydrated forms in the excited state. The transition state geometries of hydrated forms of both N9H and N7H forms of guanine in the ground state are in the zwitterionic form. This is evident from the shorter hydrogen bond distances of H \cdots O(water) bonds with that of H \cdots O6 and H \cdots N1 bonds in the ground state for both of the N9H and N7H forms (Figures 2 and 3). Thus, in the ground state, the H1 proton of guanine is significantly shifted toward the water molecule, and therefore, the water is in the form of the hydronium ion (H $_3$ O $^+$) and guanine is in the anionic form. In the case of the hydrated form of the TS-N7H transition state in the lowest singlet $\pi\pi^*$ excited state, although the H \cdots O(water) distances are increased more than the correspond-

ing ground state values, they are still smaller than the H \cdots O6 and H \cdots N1 hydrogen bond distances (these distances are decreased in the excited state as compared to the corresponding ground state values) in the excited state (Figure 3). Therefore, the hydrated TS-N7H (TS-N7H.H $_2$ O) structure remains in the zwitterionic form in the excited state, although the zwitterionic nature is decreased as compared to that in the ground state. An interesting structure is revealed for the hydrated TS-N9H (TS-N9H.H $_2$ O) form in the excited state. The H \cdots O(water) distances are significantly increased and H \cdots O6 and H \cdots N1 distances significantly decreased in the excited state as compared with the corresponding ground state values (Figure 2). Further, the H \cdots O(water) distances in the excited state are significantly larger than the H \cdots O6 and H \cdots N1 distances. Thus, hydrated TS-N9H remains in the zwitterionic form in the excited state, but in contrast to the geometry of the transition state structure in the ground state, due to the significant shift of one proton associated with water molecule toward to guanine moiety in the complex, the guanine is in the cationic form and water is in the hydroxyl anionic form.

4. Conclusions

The TD-B3LYP computed transition energies were found to be generally in good agreement with the experimental data. The ground state proton transfer reaction is characterized by a very high barrier. The inclusion of the bulk aqueous solvation using the continuum model does not decrease the barrier height. However, the inclusion of a water molecule in the proton transfer reaction path significantly decreases the barrier height. Generally, in the lowest singlet $\pi\pi^*$ excited state the proton-transfer barrier height was found to be increased. On the basis of the current theoretical calculation it appears that the singlet electronic excitation of guanine may not facilitate the excited state proton transfer corresponding to the tautomerization of the keto to the enol form. The ground state geometries of guanine tautomers including those of the transition states were found to

be planar, except for the amino group, which was pyramidal. The geometries of the keto tautomers in the lowest singlet $\pi\pi^*$ state were found to be significantly nonplanar, especially around the C6N1C2N3 part of the ring. The amino group nonplanarity was increased for the keto-N9H tautomer and decreased for the keto-N7H tautomer in the excited state. The structural nonplanarity was found to be largest for the keto-N9H tautomer. The geometries of enol tautomers were predicted to be planar, including the amino group in the excited state. The structural deformation in the TS-N9H transition state in the excited state was predicted to be different from that of the keto-N9H tautomer, whereas that for the TS-N7H transition state was predicted to be similar to the structural deformation of the keto-N7H tautomer, but to a lesser extent. Geometries of the hydrated transition states in the ground and lowest singlet $\pi\pi^*$ excited states were found to be zwitterionic in which the water molecule is in the form of a hydronium cation (H_3O^+) and guanine is in the anionic form, except for the N9H form in the excited state where the water molecule is in the hydroxyl anionic form (OH^-) and the guanine is in the cationic form.

Acknowledgment. We are thankful to financial support from NSF-CREST grant No. HRD-0318519, ONR grant No. N00034-03-1-0116, NIH-SCORE grant No. 3-S06 GM008047 31S1, and NSF-EPSCoR grant No. 02-01-0067-08/MSU. We are also thankful to the Mississippi Center for Supercomputing Research (MCSR) for the generous computational facility.

References and Notes

- (1) (a) Crespo-Hernandez, C. E.; Cohen, B.; Hare, P. M.; Kohler, B. *Chem. Rev.* **2004**, *104*, 1977. (b) Ruzsicska, B. P.; Lemaire, D. G. E. In *CRC Handbook of Organic Photochemistry and Photobiology*; Horspool, W. M., Song, P.-S., Eds.; CRC Press: New York, 1995; p 1289. (c) Eisinger, J.; Lamola, A. A. In *Excited State of Proteins and Nucleic Acids*; Steiner, R. F., Weinryb, I., Eds.; Plenum Press: New York-London, 1971. (d) Callis, P. R. *Annu. Rev. Phys. Chem.* **1983**, *34*, 329. (e) Sheina, G. G.; Stepanian, S. G.; Radchenko, E. D.; Blagoi, Yu. P. *J. Mol. Struct.* **1987**, *158*, 275. (f) Wilson, R. W.; Callis, P. R. *Photochem. Photobiol.* **1980**, *31*, 323. (g) Polewski, K.; Zinger, D.; Trunk, J.; Monteleone, D. C.; Sutherland, J. C. *J. Photochem. Photobiol. B: Biol.* **1994**, *24*, 169. (h) MacNaughton, J.; Moewes, A.; Kurmaev, E. Z. *J. Phys. Chem. B* **2005**, *109*, 7749. (i) Shugar, D.; Psoda, A. *Landolt-Bornstein's New Biophysics, Part I: Nucleic Acids*; Springer: Berlin, 1990. (j) Lin, J.; Yu, C.; Peng, S.; Aklyama, I.; Li, K.; Lee, K.; LeBreton, P. *J. Phys. Chem.* **1980**, *84*, 1006.
- (2) (a) Shukla, M. K.; Leszczynski, J. In *Computational Chemistry: Reviews of Current Trends*; Leszczynski, J., Ed.; World Scientific: Singapore, 2003; Vol. 8, p 249. (b) Leszczynski, J. In *Advances in Molecular Structure and Research*; Hargittai, M., Hargittai, I., Eds.; JAI Press: Stamford, CT, 2000; Vol. 6, p 209. (c) Leszczynski, J. In *The Encyclopedia of Computational Chemistry*; John Wiley & Sons: New York, 1998; Vol. V, p 2951. (d) Hobza, P.; Sponer, J.; Leszczynski, J. In *Computational Molecular Biology, Theoretical and Computational Chemistry Book Series*; Leszczynski, J., Ed.; Elsevier: Amsterdam, 1999; Vol. 8, p 85. (e) Sponer, J.; Hobza, P.; Leszczynski, J. In *Computational Chemistry: Reviews of Current Trends*; Leszczynski, J., Ed.; World Scientific: Singapore, 2000; Vol. 5, p 171. (f) Hanus, M.; Ryjacek, F.; Kabelac, M.; Kubar, T.; Bogdan, T. V.; Trygubenko, S. A.; Hobza, P. *J. Am. Chem. Soc.* **2003**, *125*, 7678. (g) Leszczynski, J. *Int. J. Quantum Chem.* **1992**, *19*, 43. (h) Leszczynski, J. *J. Phys. Chem. A* **1998**, *102*, 2357. (i) Shukla, M. K.; Leszczynski, J. *J. Computat. Chem.* **2004**, *25*, 768.
- (3) (a) Nir, E.; Grace, L.; Brauer, B.; de vries, M. S. *J. Am. Chem. Soc.* **1999**, *121*, 4896. (b) Nir, E.; Kleinermanns, K.; de vries, M. S. *Nature* **2000**, *408*, 949. (c) Nir, E.; Imhof, P.; Kleinermanns, K.; de vries, M. S. *J. Am. Chem. Soc.* **2000**, *122*, 8091. (d) Langer, H.; Doltsinis, N. L. *Phys. Chem. Chem. Phys.* **2004**, *6*, 2742. (e) Nir, E.; Kleinermanns, K.; Grace, L.; de Vries, M. S. *J. Phys. Chem. A* **2001**, *105*, 5106. (f) Nir, E.; Plutzer, Ch.; Kleinermanns, K.; de Vries, M. S. *Eur. Phys. J. D* **2002**, *20*, 317.
- (4) (a) Ullrich, S.; Schultz, T.; Zgierski, M. Z.; Stalow, A. *Phys. Chem. Chem. Phys.* **2004**, *6*, 2706. (b) Pecourt, J.-M. L.; Peon, J.; Kohler, B. *J. Am. Chem. Soc.* **2000**, *122*, 9348, Errata *J. Am. Chem. Soc.* **2001**, *123*, 5166. (c) Pecourt, J.-M. L.; Peon, J.; Kohler, B. *J. Am. Chem. Soc.* **2001**, *123*, 10370. (d) Kang, H.; Lee, K. T.; Jung, B.; Ko, Y. J.; Kim, S. K. *J. Am. Chem. Soc.* **2002**, *124*, 12958. (e) Canuel, C.; Mons, M.; Piuze, F.; Tardivel, B.; Dimicoli, I.; Elhaninea, M. *J. Chem. Phys.* **2005**, *122*, 74316.
- (5) (a) Nir, E.; Janzen, Ch.; Imhof, P.; Kleinermanns, K.; de Vries, M. S. *J. Chem. Phys.* **2001**, *115*, 4604. (b) Mons, M.; Dimicoli, I.; Piuze, F.; Tardivel, B.; Elhaninea, M. *J. Phys. Chem. A* **2002**, *106*, 5088. (c) Piuze, F.; Mons, M.; Dimicoli, I.; Tardivel, B.; Zhao, Q. *Chem. Phys. Lett.* **2001**, *270*, 205. (d) Chin, W.; Mons, M.; Dimicoli, I.; Piuze, F.; Tardivel, B.; Elhaninea, M. *Eur. Phys. J. D* **2002**, *20*, 347.
- (6) (a) Shukla, M. K.; Mishra, S. K.; Kumar, A.; Mishra, P. C. *J. Comput. Chem.* **2000**, *21*, 826. (b) Langer, H.; Doltsinis, N. L. *J. Chem. Phys.* **2003**, *118*, 5400. (c) Mennucci, B.; Toniolo, A.; Tomasi, J. *J. Phys. Chem. A* **2001**, *105*, 7126.
- (7) Gorb, L.; Leszczynski, J. *J. Am. Chem. Soc.* **1998**, *120*, 5024.
- (8) (a) Scheiner, S. *J. Phys. Chem. A* **2000**, *104*, 5898. (b) Catalan, L.; Perez, P.; del Valle, J. C.; de Paz, J. L. G.; Kasha, M. *Proc. Natl. Acad. Sci. U.S.A.* **2004**, *101*, 419. (c) Sobolewski, A. L.; Domcke, W. *Chem. Phys. Lett.* **1999**, *300*, 533.
- (9) (a) Casida, M. E.; Jamorski, C.; Casida, K. C.; Salahub, D. R. *J. Chem. Phys.* **1998**, *108*, 4439. (b) Stratmann, R. E.; Scuseria, G. E.; Frisch, M. J. *J. Chem. Phys.* **1998**, *109*, 8218. (c) Wiberg, K. B.; Stratmann, R. E.; Frisch, M. J. *Chem. Phys. Lett.* **1998**, *297*, 60. (d) Hirata, S.; Head-Gordon, M. *Chem. Phys. Lett.* **1999**, *314*, 291.
- (10) Foresman, J. B.; Head-Gordon, M.; Pople, J. A.; Frisch, M. J. *J. Phys. Chem.* **1992**, *96*, 135.
- (11) (a) Cancès, M. T.; Mennucci, B.; Tomasi, J. *J. Chem. Phys.* **1997**, *107*, 3032. (b) Cossi, M.; Barone, V.; Mennucci, B.; Tomasi, J. *Chem. Phys. Lett.* **1998**, *286*, 253. (c) Cossi, M.; Scalmani, G.; Rega, N.; Barone, V. *J. Chem. Phys.* **2002**, *117*, 43.
- (12) Frisch, M. J.; Trucks, G. W.; Schlegel, H. B.; Scuseria, G. E.; Robb, M. A.; Cheeseman, J. R.; Montgomery, J. A., Jr.; Vreven, T.; Kudin, K. N.; Burant, J. C.; Millam, J. M.; Iyengar, S. S.; Tomasi, J.; Barone, V.; Mennucci, B.; Cossi, M.; Scalmani, G.; Rega, N.; Petersson, G. A.; Nakatsuji, H.; Hada, M.; Ehara, M.; Toyota, K.; Fukuda, R.; Hasegawa, J.; Ishida, M.; Nakajima, T.; Honda, Y.; Kitao, O.; Nakai, H.; Klene, M.; Li, X.; Knox, J. E.; Hratchian, H. P.; Cross, J. B.; Adamo, C.; Jaramillo, J.; Gomperts, R.; Stratmann, R. E.; Yazyev, O.; Austin, A. J.; Cammi, R.; Pomelli, C.; Ochterski, J. W.; Ayala, P. Y.; Morokuma, K.; Voth, G. A.; Salvador, P.; Dannenberg, J. J.; Zakrzewski, V. G.; Dapprich, S.; Daniels, A. D.; Strain, M. C.; Farkas, O.; Malick, D. K.; Rabuck, A. D.; Raghavachari, K.; Foresman, J. B.; Ortiz, J. V.; Cui, Q.; Baboul, A. G.; Clifford, S.; Cioslowski, J.; Stefanov, B. B.; Liu, G.; Liashenko, A.; Piskorz, P.; Komaromi, I.; Martin, R. L.; Fox, D. J.; Keith, T.; Al-Laham, M. A.; Peng, C. Y.; Nanayakkara, A.; Challacombe, M.; Gill, P. M. W.; Johnson, B.; Chen, W.; Wong, M. W.; Gonzalez, C.; Pople, J. A. *Gaussian 03, Revision B.03*; Gaussian, Inc.: Pittsburgh, PA, 2003.
- (13) Flükiger, P.; Lüthi, H. P.; Portmann, S.; Weber, J. *MOLEKEL 4.3*; Swiss Center for Scientific Computing, Manno (Switzerland), 2000, www.cscs.ch/molekel.
- (14) (a) Voet, D.; Gratzner, W. B.; Cox, R. A.; Doty, P. *Biopolymers* **1963**, *1*, 193. (b) Matsuoka, Y.; Norden, B. *J. Phys. Chem.* **1982**, *86*, 1378. (c) Clark, L. B. *J. Am. Chem. Soc.* **1994**, *116*, 5265. (d) Yamada, T.; Fukutome, H. *Biopolymers* **1968**, *6*, 43.
- (15) Fulscher, M. P.; Serrano-Andres, L.; Roos, B. O. *J. Am. Chem. Soc.* **1997**, *119*, 6168.
- (16) Wilson, R. W.; Morgan, J. P.; Callis, P. R. *Chem. Phys. Lett.* **1975**, *36*, 618.